The identification, characterization, and management of *Rotylenchulus reniformis* on *Cucumis melo* in China

Qianqian Shi[1†] , Xinyue Cai[1†], Ziqi Zhang[1], Wenwen Song[1], Chen Liang[1], Fangmeng Duan[1] and Honghai Zhao[1*]

Abstract

The reniform nematode, *Rotylenchulus reniformis*, is a sedentary root parasite that poses a significant threat to agricultural production in tropical and subtropical regions worldwide. In 2021–2022, a population of *R. reniformis* was identified in a melon greenhouse in Jimo District, Qingdao, China. To characterize this population, we employed morphological, morphometric, and molecular methods, which confirmed the identity of the nematodes as *R. reniformis*. Our investigation revealed that *R. reniformis* successfully infected the roots of melon plants and laid eggs, which could have led to significant crop damage. This report represents the first documented example of *R. reniformis* infecting melon plants in China. We evaluated several control strategies to combat this nematode, and our results indicated that soil solarization and the use of fosthiazate or chitooligosaccharide copper in combination with soil solarization were effective measures for managing *R. reniformis* in a greenhouse setting. In addition, combining soil solarization with chitooligosaccharide copper promoted melon plant growth and increased the relative abundance of microorganisms with biocontrol potential.

Keywords *Rotylenchulus reniformis*, Melon plants, Control, Rhizosphere microbiota

Background

Melon (*Cucumis melo*), also known as cantaloupe or muskmelon, is a highly valued crop cultivated in temperate and tropical regions worldwide. China is a leading producer of melons, accounting for approximately 35% of global production, with a yield of 13.87 million tons (FAOSTAT 2020). This fruit is a popular choice for consumers due to its delicious flavor, texture, and taste. Furthermore, several studies have demonstrated that melon

is a rich source of health-promoting compounds, including carotenoids, folic acid, polyphenols, vitamins C, and minerals (Maietti et al. 2012; Rodriguez-Perez et al. 2013; Rico et al. 2020). Moreover, melons have potential applications as skin moisturizers and stomachic agents (Ritschel et al. 2004).

Plant-parasitic nematodes (PPNs) are a global problem in the agricultural industry due to the damage they cause to crops and their role in spreading pathogens such as fungi and viruses (Pulavarty et al. 2021; Shao et al. 2023). There are over 4100 species of PPNs described in the literature, and according to surveys of researchers, the reniform nematode (RN) is considered as one of the top 10 PPNs based on its economic impact and scientific importance (Jones et al. 2013). RNs can infect the roots of more than 300 plant species, including cotton, soybean, pineapple, and olive

†Qianqian Shi and Xinyue Cai have contributed equally to this work.

*Correspondence:
Honghai Zhao
hhzhao@qau.edu.cn
[1] Shandong Engineering Research Center for Environment-Friendly Agricultural Pest Management, College of Plant Health and Medicine, Qingdao Agricultural University, Qingdao 266109, China

Shi *et al. Phytopathology Research*   (2023) 5:58

Page 2 of 14

(Robinson et al. 2005; Wubben et al. 2010; Nguyen et al. 2020). Reniform nematodes are mostly found in tropical and warm temperate regions of the world, and they are distributed throughout southern China (Zhang 2010). Infection by *R. reniformis* results in plant stunting, chlorosis, and yield reduction (Robinson et al. 2005; Nguyen et al. 2020). Moreover, plants infected by *R. reniformis* often present with disease complexes involving other soil-borne pathogens, such as *Fusarium solani*, *Verticillium* spp., and *Rhizoctonia solani*, leading to even greater losses (Castillo et al. 2010). Compared with most PPNs, *R. reniformis* is widely adapted to different soil types, including soils with high silt and clay content, and can colonize deep in the soil and maintain an anhydrobiotic state to survive the winter (Robinson 2007). All of these characteristics make it challenging to eliminate this nematode from infested soils. The identification of the reniform nematode species, distribution, and its host range is fundamentally important to effective integrated management.

Various strategies have been developed to manage RNs (Davis et al. 2003; Usovsky et al. 2021), but the most common approach has been the application of chemical nematicides. However, these nematicides are not only expensive but also harmful to the environment and human health (Koenning et al. 2004; Chen et al. 2020). Due to their negative environmental and human health impact, many chemical nematicides like methyl bromide and dibromochloropropane have been banned in agriculture (Noling and Becker 1994; Schneider et al. 2003). To promote healthy and high-quality food production using environmentally friendly, low-cost, and effective methods, integrated pest management (IPM) strategies that combine multiple tactics have been proposed for RN control, such as judicious use of soil solarization and genotype (Chellemi et al. 1993). These sustainable methods can help minimize the use of chemical nematicides while ensuring efficient control of RNs.

In 2021–2022, *R. reniformis* was detected in the roots of some irregular stunted melon plants (Additional file 1: Figure S1) and rhizosphere soil in the Jimo District of Qingdao, China. The nematode was identified and characterized using a combination of morphological, morphometric, and molecular methods. Furthermore, we investigated the efficacy of soil solarization independently and in combination with fosthiazate or chitooligosaccharide copper treatments to control *R. reniformis* infection in melon plants under greenhouse conditions. To our knowledge, this is the first report of *R. reniformis* in *C. melo* in China, and our findings now lay a foundation for effective management strategies for *R. reniformis* in greenhouse settings.

Results

Morphological and morphometric characteristics of the nematode

As shown in Table 1, the morphological traits of the *R. reniformis* population in this study mostly fall within the range of variation in previous studies (Agudelo et al. 2005; Lopez-Nicora et al. 2018; Liu et al. 2023a). The immature female body had a C-shaped form (Fig. 1a), a high and conoid-rounded lip region that blended smoothly with the body contour. It also had a long, well-developed stylet with rounded knobs that slope towards the posterior (Fig. 1b). The vulva was located at the posterior end, between 66.7 and 72.1% of the body length (mean = 71.3%) (Fig. 1a). The body shape of the male was like that of the immature female with a reduced stylet (Fig. 1c, d) and well-developed spicule and gubernaculum (Fig. 1e). The mature female body was kidney-shaped with a well-formed vulva, which had two raised lips and a tail that had a finger-like tip with a prolonged hyaline portion (Fig. 1f).

Molecular characterization of the nematode

PCR amplification of the D2–D3 region of the 28S and the ITS1 rRNA gene was performed on the nematode sample described above. Four new sequences of 28S rRNA gene (accession number: OR399163, OR399166, OR404988, and OR404989) and six new sequences of ITS1 in the rRNA gene (OR418490, OR418491, and OR432066–OR432069) were obtained in the present study. The intraspecific variability among the D2–D3 region of the 28S from *R. reniformis* was found to be considerably high, ranging from 85 to 98%. Sequences of OR399163 and OR399166 (28S rRNA gene) showed similarity values of > 98% with other identified sequences of *R. reniformis* deposited in the National Center for Biotechnology Information (NCBI) database from the USA (KT003743 and KT003746), and sequences of OR404988 and OR404989 (28S rRNA gene) showed similarity values of > 96% with other identified sequences of *R. reniformis* deposited in the NCBI database from China (KP054112 and KP054128). Sequences of OR418490, OR418491, and OR432069 (ITS1 rRNA gene) showed similarity values of > 98% with other identified sequences of *R. reniformis* deposited in the NCBI database from China (GU003948 and KP018567), and sequences of OR432066–OR432068 (ITS1 rRNA gene) showed similarity values of > 98% with other identified sequences of *R. reniformis* deposited in the NCBI database from China and Japan (GU003962, LC335935, and LC335911).

A phylogenetic tree was constructed using four new D2–D3 sequences in this study and 64 other 28S rRNA gene sequences. *R. reniformis* is divided into two clades: type A and type B, showing a sister relationship

Shi *et al. Phytopathology Research* (2023) 5:58

Page 3 of 14

Table 1 Morphometrics of females and males from the *R. reniformis* isolate

Character	Melon plants, Shandong province, China		Olive, Spain (Palomares-Rius et al. 2018)		Cotton, Limestone, Alabama, USA (Agudelo et al. 2005)		Sponge gourd, Yunnan province, China (Liu et al. 2023)	
	Immature females	Males	Immature females	Males	Immature females	Males	Immature females	Males
n	20	20	10	10	20	20	20	20
L	420.6±34.2 (351.8–474.1)	427.8±28.1 (356.3–495.5)	464±30.5 (378–469)	438±27.7 (398–486)	399.8 (365–425)	404.3 (375–445)	392.3±20.4 (352.8–436.7)	426.7±31.0 (368.1–463.9)
W	16.9±0.9 (14.8–18.6)	15.7±1.2 (14.0–19.6)	17.7±0.8 (16.0–19.0)	20.3±0.9 (19.0–22.0)	16.9 (15–19)	14.4 (13–17)	–	–
a	24.8±1.5 (22.4–27.8)	27.3±1.2 (21.8–30.9)	24.7±1.9 (21.0–27.4)	21.6±0.9 (20.4–23.4)	23.7 (21.1–26.6)	28.2 (24.1–31.9)	25.2±1.1 (23.5–27.3)	27.7±2.2 (25.2–30.7)
ST	16.0±0.9 (13.6–17.3)	11.5±1.1 (9.9–14.9)	16.7±0.7 (16.0–18.0)	12.5±0.7 (11.0–13.0)	19.2 (17–20)	15.1 (13–18)	18.6±0.5 (17.6–19.4)	12.8±0.8 (11.2–14.1)
DGO	14.9±1.1 (13.1–17.2)	16.7±0.9 (14.9–17.9)	14.5±1.1 (13.0–16.0)	17.2±0.8 (16.0–18.0)	–	–	–	–
H-Ep	87.1±4.6 (79.3–95.9)	80.1±4.2 (70.8–89.6)	76.4±5.8 (70.0–90.0)	91.8±7.1 (80.0–98.0)	88.3 (75–100)	81.2 (70–95)	–	–
Oes	120.8±10.0 (96.8–135.6)	99.8±7.6 (80.2–114.3)	–	–	128 (110–150)	110.0 (95–125)	–	–
b	3.5±0.3 (2.9–4.5)	4.3±0.2 (3.8–4.8)	–	–	3.1 (2.6–3.5)	3.7 (3.3–4.1)	3.2±0.4 (2.6–4.0)	4.5±0.4 (3.9–4.8)
AM	63.5±3.3 (58.1–68.4)	59.1±6.0 (48.9–67.5)	–	–	–	–	–	–
V	71.7±1.6 (67.2–74.6)	–	70.8±1.7 (68.0–73.0)	–	–	–	70.3±1.0 (68.5–72.6)	–
V.a	90.7±9.9 (72.4–111.3)	–	–	–	–	–	–	–
ABW	9.6±0.8 (7.9–10.9)	9.3±0.8 (8.1–10.9)	9.7±0.7 (9.0–11.0)	8.8±0.6 (8.0–10.0)	10.7 (9–13)	10.65 (9–12)	–	–
VBW	16.2±0.9 (14.3–17.6)	–	–	–	–	–	–	–
Tail	26.9±2.9 (22.3–35.6)	25.4±2.6 (22.6–31.9)	23.3±1.6 (22.0–26.0)	26.4±1.6 (24.0–28.0)	28.9 (18–40)	28 (24–32)	25.9±2.2 (20.1–29.9)	26.3±1.8 (24.3–29.4)
c	15.7±1.2 (13.3–18.7)	16.9±1.6 (13.4–19.7)	18.8±1.5 (16.6–21.3)	16.6±0.8 (15.3–17.4)	14.3 (10–22.8)	14.5 (13.0–16.9)	15.2±1.2 (13.6–18.6)	15.5±0.9 (14.7–16.8)
c'	2.8±0.3 (2.4–3.3)	2.7±0.3 (2.1–3.5)	2.4±0.2 (2.2–2.9)	3.0±0.3 (2.7–3.5)	2.7 (2.0–3.5)	2.6 (2.2–3.3)	2.9±0.3 (2.2–3.3)	2.8±0.3 (2.5–3.2)
Spi	–	20.3±1.4 (18.6–23.1)	–	20.8±1.3 (19.0–23.0)	–	20.4 (18–24)	–	20.6±0.9 (19.6–22.7)

All measurements are expressed as means±SD (range) with units in µm

Abbreviations of morphological features. L: Body length; W: Greatest body width; a: Body length divided by greatest body width; ST: Stylet length; DGO: Dorsal gland orifice to stylet; H-Ep: Distance from excretory pore to anterior end; Oes: Oesophagus length; b: body length divided by oesophageal length; AM: Distance from anterior end to center of median oesophageal bulb valve; V: Distance from head end to vulva×100 divided by body length; V. a: Distance from vulva to anus; ABW: Anal body width; VBW: Vulval body width; Tail: Tail length; c: Body length divided by tail length; c': Tail length divided by body width at anus; Spi: Spicules length

with *R. macrodoratus*. Two new sequences in this study (OR399163 and OR399166) are clustered in the type A clade, and another two new sequences (OR404988 and OR404989) are clustered in the type B clade (Fig. 2). Similar to the D2–D3 tree, ITS1 in the rRNA genes from *R. reniformis* population in this study also formed two different subclades. Three new sequences in this study (OR418490, OR418491, and OR432069) are clustered in the type A clade and other three new

sequences (OR432066–OR432068) are clustered in the type B clade (Fig. 3).

Assessing melon plant roots for infection by the isolated *R. reniformis*

We inoculated the roots of melon plants with the newly hatched J2s of *R. reniformis* and observed successful penetration at 4 days post-inoculation (dpi). Females protruding from the roots appeared swollen at 7 dpi,
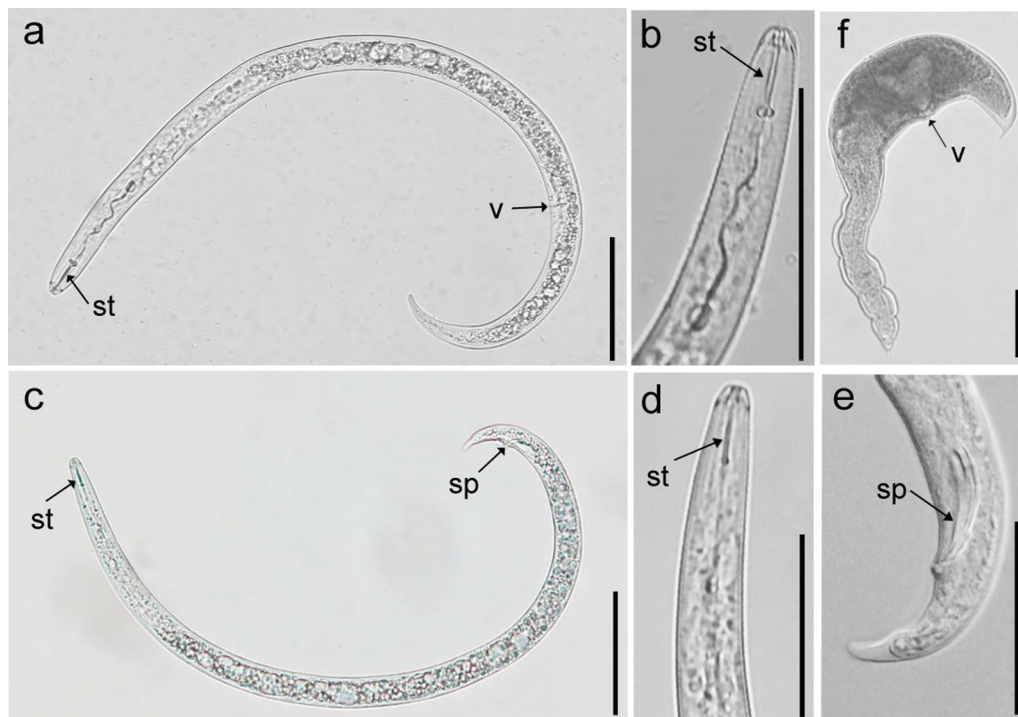
Fig. 1 The morphological characteristics of *R. reniformis* from *C. melo* from a Shandong province greenhouse observed using a compound microscope. Image panels contain pictures of **a** an immature female, **b** the anterior part of an immature female, **c** a male, **d** the anterior part of a male, **e** the spicule of a male, and **f** mature females. st = stylet, v = vulva, sp = spicule. Scale bars = 50 μm

and their bodies became kidney-shaped by 10 dpi. The females laid eggs at 15 dpi (Additional file 1: Figure S2). Then, the egg masses were hand-picked from the roots and placed in Petri dishes containing sterilized water. Hatched J2s of *R. reniformis* were detected at 3 days after incubation. The results verified that our isolate of *R. reniformis* could successfully infect the roots of melon plants and complete its life cycle within 18 days at a temperature of $26 \pm 3°C$.

Population dynamics of the *R. reniformis* and its response to common control strategies in the greenhouse

The greenhouse was highly infested with *R. reniformis* with an original average population density of 574.2 ± 15.3 and 345.7 ± 18.4 nematodes/100 g of soil in 2021 and 2022, respectively. In 2021, after the transplanting of melon plants in greenhouse plots, the infection of *R. reniformis* was monitored in the root system. The number of infected *R. reniformis* peaked 8 days after transplanting (October 2nd), with an average nematode density of 1140.3 ± 89.2 nematodes/10 g of roots. The nematode density then began to decline before increasing again and peaking at 93.0 ± 5.9 nematodes/10 g of roots at 23 days after transplanting (October 17th) (Fig. 4a). The density of *R. reniformis* in the rhizosphere gradually increased from September to December when it reached a peak density

of 2269.3 ± 72.3 nematodes/100 g of soil nearly three months after transplanting (December 14th) (Fig. 4b). A similar population dynamics of the *R. reniformis* in melon plants roots and rhizosphere was detected in 2022 (Fig. 4c, d).

We then tested the efficacy of different potentially nematicidal treatments against *R. reniformis*. Soil solarization (S), fosthiazate (F), a combination of soil solarization and fosthiazate (SF), or a combination of soil solarization and chitooligosaccharide copper (SC) were all used as treatments against *R. reniformis* in greenhouse assays. All four treatments resulted in reduced nematode infection in melon plant roots and the rhizosphere compared with the blank control (BC) in 2021 and 2022 (Fig. 4). The SF and SC treatments led to significantly reduced *R. reniformis* infection compared to the F and BC treatments ($P < 0.05$). In 2021, the S and F treatments resulted in 98.1% and 78.2% reductions in nematode density, respectively, compared to the BC treatment when root samples were taken 8 days after transplanting (October 2nd). The SF and SC treatments were the most effective and nearly eliminated nematodes from melon plant roots 8 days after transplanting (October 2nd) (Fig. 4a). The F treatment initially reduced *R. reniformis* in the rhizosphere soil two weeks after transplanting, but this effect reversed
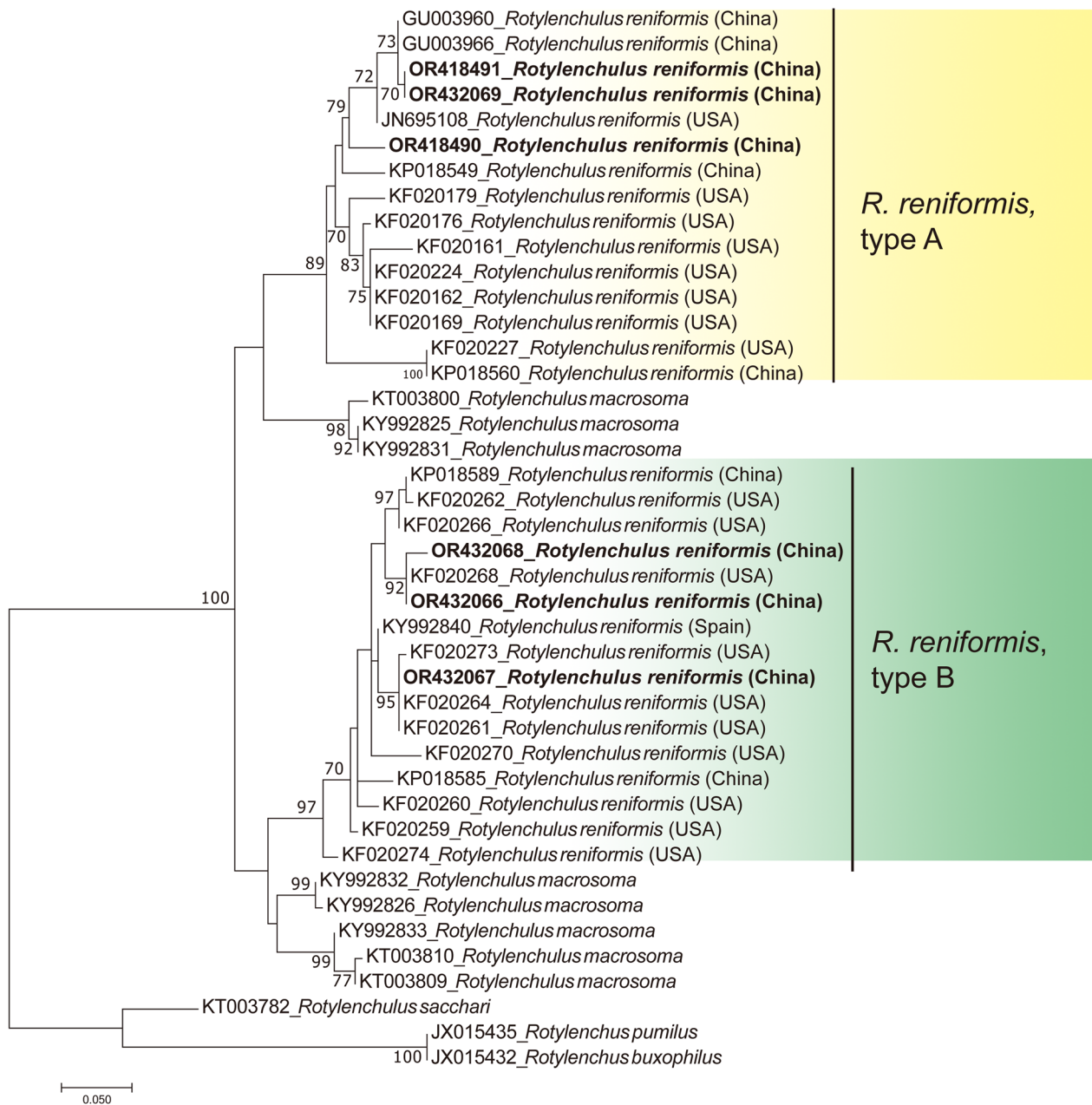
Fig. 2 A phylogenetic tree based on the alignment of sequences from the D2–D3 region of the 28S rRNA gene of *R. reniformis* isolated from *C. melo* and other *Rotylenchulus* species. The phylogenetic tree was constructed using the maximum likelihood method supported by bootstrap for 1000 replicates. The bootstrap value is given on each node. Four bold marked sequences (OR399163, OR399166, OR404988, and OR404989) were from this study

Shi *et al. Phytopathology Research*   (2023) 5:58

Page 6 of 14

Fig. 3 A phylogenetic tree based on the alignment of sequences from the ITS1 rRNA gene of *R. reniformis* isolated from *C. melo* and other *Rotylenchulus* species. The phylogenetic tree was constructed using the maximum likelihood method supported by bootstrap for 1000 replicates. The bootstrap value is given on each node. Six bold marked sequences (OR418490, OR418491, and OR432066–OR432069) were from this study

as nematodes proliferated during the middle and later part of the growing season (Fig. 4b). In 2022, compared with the BC treatment when root samples were taken 10 days after transplanting (October 12th), the S, F, SF, and SC treatments decreased nematodes in the infected roots by 98.2%, 91.3%, 100%, and 100%, respectively. The melon plants treated with S, particularly the combinations of SF and SC, had fewer *R. reniformis* in the

rhizosphere soil throughout the growing season compared to the other treatments (Fig. 4b, d).

We also measured plant growth parameters (shoot weight and shoot length) of melon plants under different treatment conditions. We found that the SC treatment was the most effective in promoting melon plant growth. In 2021, the shoot weight was approximately twice as high as the BC, whereas the shoot length was 60% higher
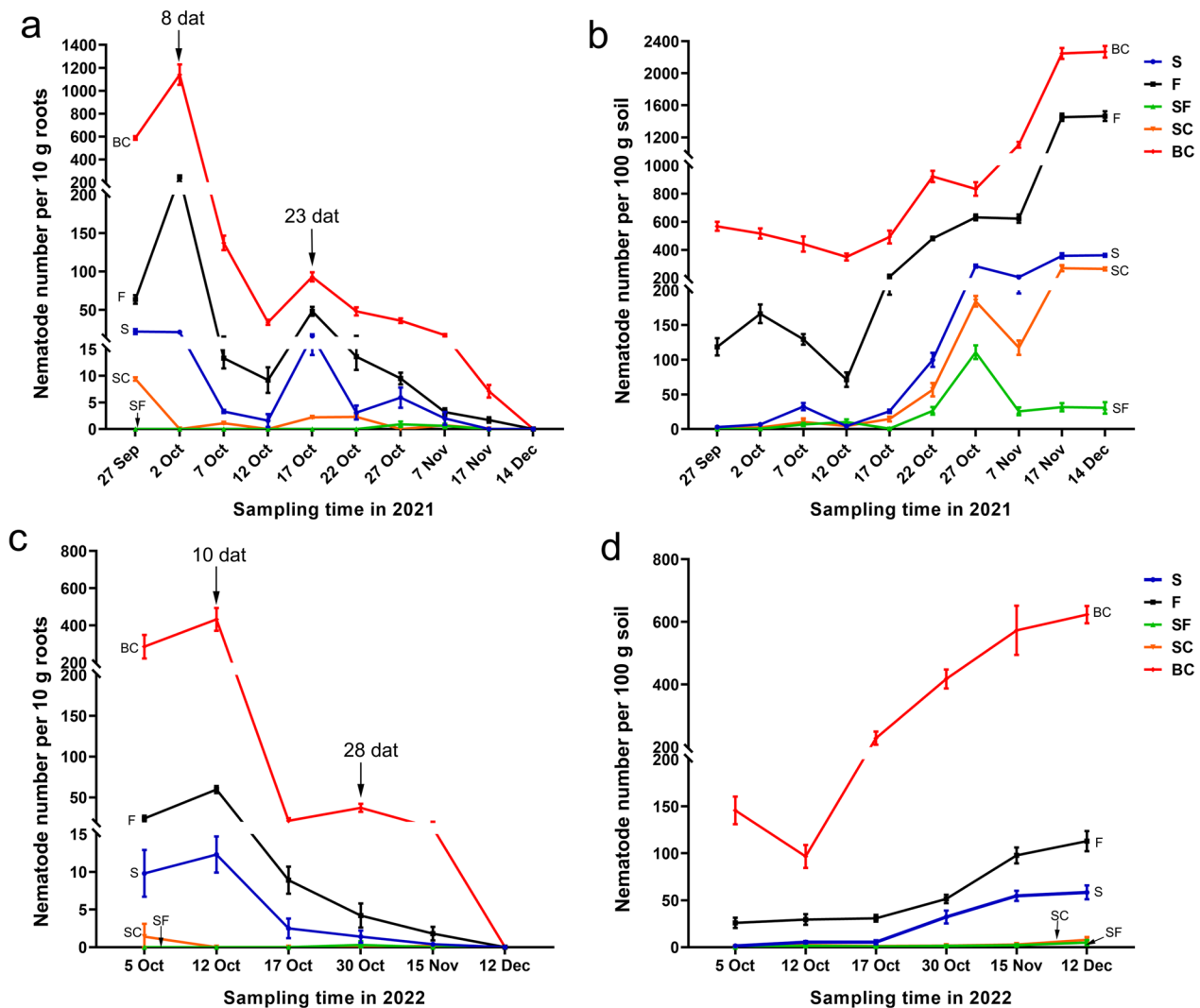
Shi *et al. Phytopathology Research*   (2023) 5:58

Page 7 of 14

Fig. 4 Population dynamics of *R. reniformis* and treatment efficacy in greenhouse experiments in the years 2021 and 2022. **a** The population density of *R. reniformis* on *C. melo* roots under different treatments in 2021. **b** The population density of *R. reniformis* in the rhizosphere soil of *C. melo* under different treatments in 2021. **c** The population density of *R. reniformis* on *C. melo* roots under different treatments in 2022. **d** The population density of *R. reniformis* in the rhizosphere soil of *C. melo* under different treatments in 2022. The *C. melo* plants were transplanted into infested soil on September 24th, 2021 and October 2nd, 2022. The number of *R. reniformis* in *C. melo* roots and rhizosphere soil was recorded 3 days after the transplanting of *C. melo* seedlings. S: soil solarization; F: fosthiazate; SF: combination of soil solarization and fosthiazate; SC: combination of soil solarization and chitooligosaccharide copper; BC: blank control; dat: days after transplanting

than the BC. We also detected a significant increase in the shoot weight and length after SC treatment in 2022 (Additional file 2: Table S1).

The effects of S and SC treatments on the rhizosphere microbiota

Melon plants treated with S clearly (Fig. 4) had fewer *R. reniformis* nematodes in their roots than plants treated with F. The combination treatment of SC, which involved the use of S and chitooligosaccharide copper, proved effective in controlling *R. reniformis* and contributed

to improved plant growth. We next evaluated the effect of S and SC treatments on the rhizosphere microbiota by measuring the relative abundance of soil microbial communities at the genus level. Unidentified Gemmatimonadaceae, Vicinamibacterales, Vicinamibacteraceae, and *Sphingomonas* were the dominant bacteria in all rhizosphere soils (Fig. 5a and Additional file 2: Table S2). The three most abundant fungi were from unidentified Basidiomycota, *Xeromyces*, and *Cladosporium* (Fig. 5b and Additional file 2: Table S3). To determine the alpha diversity of rhizosphere microbiota, the Shannon index
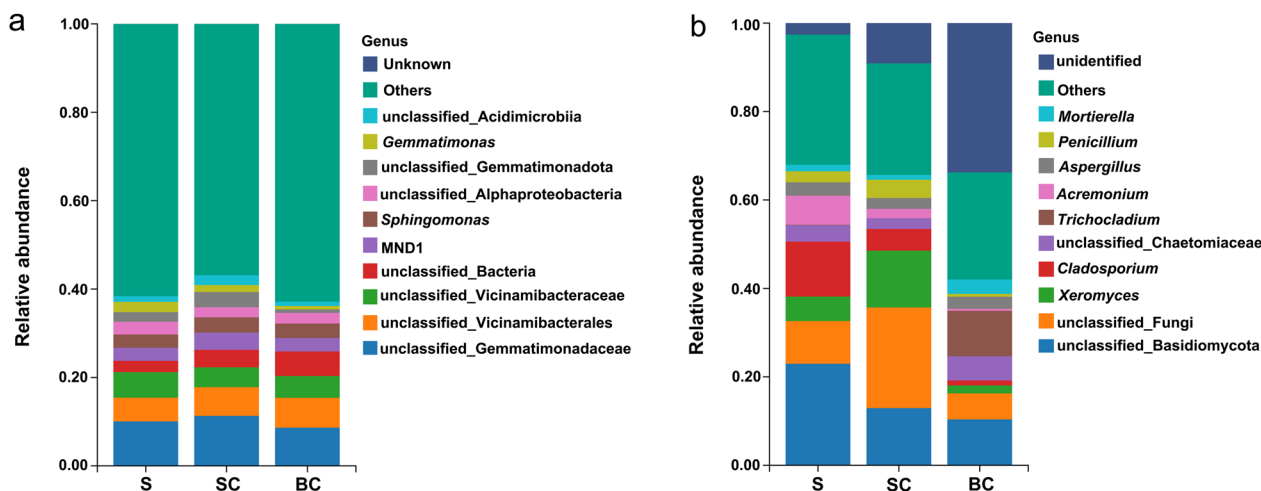
Fig. 5 The relative abundance of rhizosphere microbiota in the rhizosphere soil of *C. melo*. The relative abundance of **a** bacteria, and **b** fungi at the genus level

(reflecting species richness) and abundance-based richness estimation (ACE, reflecting species abundance) indexes were calculated. The results showed that the Shannon index of bacteria in S and SC was significantly lower than that in BC, but there was no significant difference between the ACE indexes of bacteria in the rhizosphere treated with SC and BC. However, a pronounced decline in the ACE index was observed with the S treatment. Both the S and SC treatments significantly increased the Shannon index of fungi, whereas no significant differences were observed in the ACE index between S, SC, and BC treatments. A principal coordinate analysis (PCoA) showed significant differences in the structure of bacterial and fungal communities in the rhizosphere treated with S, SC, and BC (Additional file 1: Figure S3).

The Gram-staining phenotypes of microbiota were predicted by BugBase (Fig. 6a, b). An integrated ANOVA analysis was conducted to examine the relative abundance of *Bacillus* spp. within the gram-positive bacteria. The results indicated that soils treated with SC had a higher relative abundance of *Bacillus* spp. compared to those treated with BC (Fig. 6c). We also used high-dimensional biomarkers to group fungal communities at the genus level in the rhizosphere treated with S, SC, and BC by ANOVA analysis. The relative abundance of the 18 most abundant genera of fungi in rhizosphere treated with S, SC, and BC is shown in Fig. 7. Certain fungi with potential biocontrol activity, such as *Penicillium*, *Polypaecilum*, *Gibellulopsis*, *Wickerhamomyces*, and *Hannaella*, were significantly more abundant in the rhizosphere treated with S and SC (Fig. 7). Inversely, the abundance of potentially plant pathogenic fungi, such as *Fusarium* and *Metacordyceps*, were
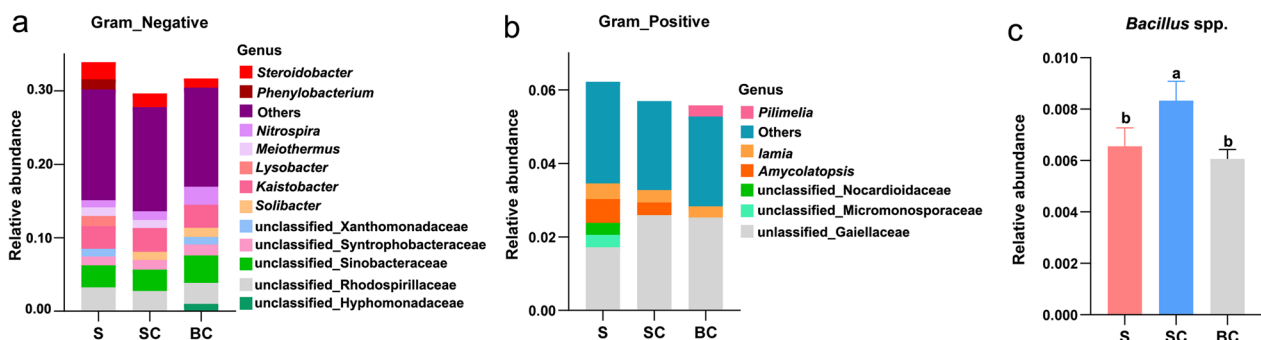

Fig. 6 Microbial community phenotypes and bacterial community composition in the rhizosphere soil of *C. melo* based on BugBase prediction. **a**, **b** Classification of bacteria based on Gram staining. **c** The relative abundance of *Bacillus* spp. in the rhizosphere of soils treated with BC, S, or SC. Each bar represents the mean ± SD. The different lowercase letters on the bars indicate significant differences according to one-way ANOVA ($P < 0.05$, Tukey's HSD test). BC: blank control; S: soil solarization; SC: combination of soil solarization and chitooligosaccharide copper
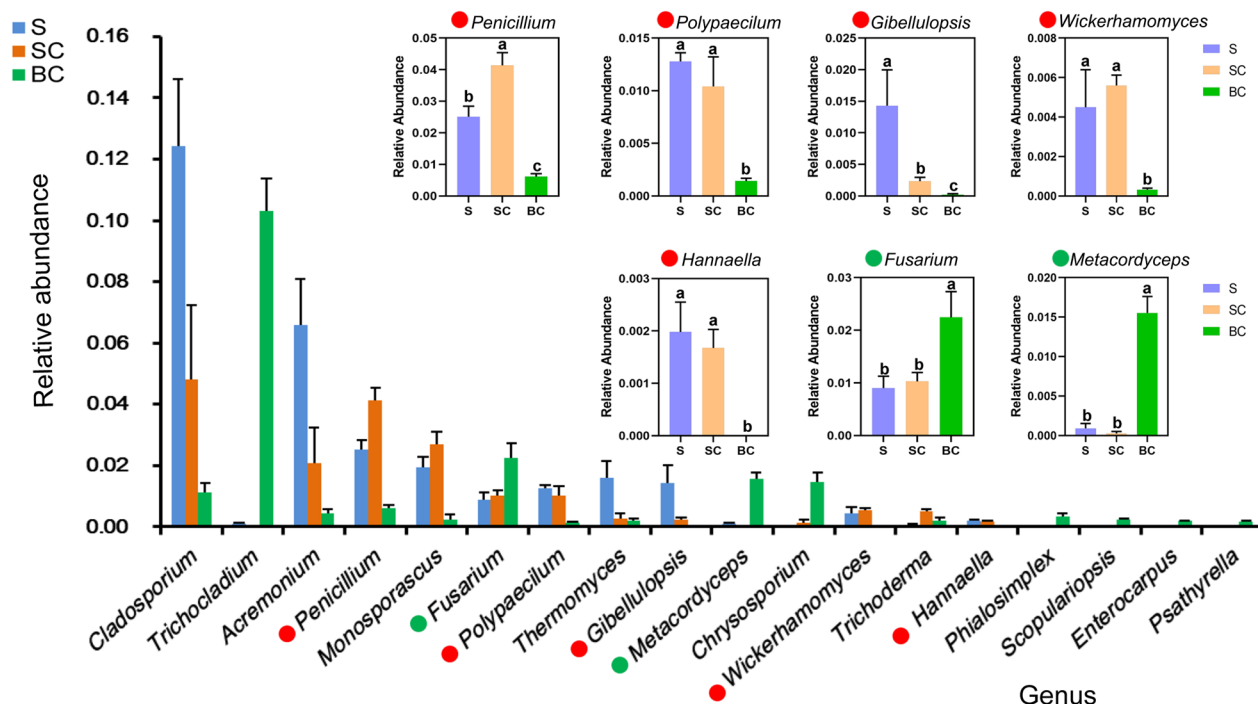
Shi *et al. Phytopathology Research*   (2023) 5:58

Page 9 of 14

Fig. 7 The relative abundance of the 18 most abundant genera of fungi in the rhizosphere soil of *C. melo* treated with S, SC, or BC. The red solid circles denote fungi with plant disease biocontrol potential. The green solid circles denote fungi with plant pathogenic potential. Each bar represents the mean ± SD. The different lowercase letters on the bars indicate significant differences according to one-way ANOVA ($P < 0.05$, Tukey's HSD test). S: soil solarization; SC: combination of soil solarization and chitooligosaccharide copper; BC: blank control

significantly less abundant in the rhizosphere treated with S and SC (Fig. 7).

Discussion

R. reniformis is a parasitic nematode that can infect a wide range of crops and vegetables, leading to severe damage and significant yield losses in agriculture. In this study, we first report the occurrence of *R. reniformis* on melon plants in China and provide detailed morphological and molecular characterizations of this species. Moreover, we also assessed the population dynamics of *R. reniformis* in the greenhouse and evaluated the efficacy of several control strategies.

There are several tools available to identify different species of *Rotylenchulus*. However, distinguishing between species based on their physical characteristics is not very effective due to the high variability of some features in *Rotylenchulus*. Ribosomal RNA genes have been used effectively in molecular diagnostics to uncover the diversity within the *Rotylenchulus* genus (Van Den Berg et al. 2016; Palomares-Rius et al. 2018). Intraspecific and intra-individual rRNA variation is commonly found in the genus *Rotylenchulus*. There is evidence that higher rRNA polymorphisms are associated with increased growth and reproduction (Elser et al. 2000), and Qing

et al. (2020) suggested that the rRNA copy number in *R. reniformis* may still be expanding. In the present study, we found two distinct types of 28S and ITS from *R. reniformis*, which is consistent with the findings of previous research by Van Den Berg et al. (2016) and Palomares-Rius et al. (2018).

In China, *R. reniformis* has been reported in the southern regions of Shanghai, Guangdong, Guangxi, Hainan, Anhui, Sichuan, Fujian, Guizhou, Jiangxi, Hubei, Zhejiang, and Yunnan (Zhang 2010; Liu et al. 2023a), posing a serious threat to the production of cotton, banana, citrus fruits, and vegetables in those areas. To our knowledge, this is the first report of *R. reniformis* on melon plants in China. In other part of the world, we only found reports about the infection of *R. reniformis* in melon plants in Brazil, which caused high yield losses of melon when there were high population densities of the reniform nematode in the field (Moura et al. 2002). Gustavo et al. (2005) evaluated the resistance of eight cucurbit genotypes to *R. reniformis* under greenhouse conditions and found that *R. reniformis* presented high reproduction in two tested *C. melon* varieties. Similarly, our study showed that *R. reniformis* can reproduce in the roots of the melon plants and complete its life cycle within 18 days, which

is similar to that reported for *R. reniformis* on susceptible soybean (19 days) (Rebois 1973) and cotton (17 days) (Robinson 2007). In some areas of the USA, the reniform nematodes caused greater loss than root-knot nematodes due to the shorter life cycle and higher reproductive rate (Robinson 2007). The potential damage of *R. reniformis* necessitates strict testing to detect *R. reniformis* before seedling transportation, especially in greenhouse planting areas of China, to avoid great losses in vegetable production.

There is also an urgent need to determine the efficacy of environmentally friendly control methods to prevent the spread of *R. reniformis* and ensure the sustainable development of the vegetable industry. We evaluated the ability of S, F, SF, and SC treatments to control *R. reniformis* in the greenhouse. Chitooligosaccharide is the degradation product of chitosan, the second most abundant polymer in nature after cellulose (Fan et al. 2023). Previous studies have reported that chitooligosaccharide has antifungal, antibacterial, and plant growth promotion properties and can enhance plant disease resistance (Guan and Feng 2022; Liu et al. 2023b). Chitooligosaccharide and its modified derivatives have been widely used in agriculture due to their excellent biocompatibility and low cost (Fan et al. 2022; Liu et al. 2023b). In this study, we found that soil solarization had a significant effect on the population of *R. reniformis*, which was consistent with a previous report (Chellemi et al. 1993). Moreover, combining soil solarization with fosthiazate or chitooligosaccharide copper had the greatest efficacy in eliminating nematodes from melon plant roots and rhizosphere soil. Additionally, the application of chitooligosaccharide copper after soil solarization can significantly improve melon plant growth.

Many studies have demonstrated that soil microbial communities influence plant growth and disease resistance under biotic and abiotic stress. Our microbiome analysis showed that treating soil with SC significantly increased the abundance of *Bacillus*. *Bacillus* species such as *B. cereus*, *B. subtilis*, *B. megaterium*, and *B. velezensis* have been previously shown to provide effective control against PPNs in field experiments, with some species even promoting plant growth (Cao et al. 2019; Yin et al. 2021; Zhou et al. 2021; Tian et al. 2022). For example, the *B. velezensis* strain Bv-DS1 isolated from tidal soil can suppress *M. incognita* infection in tomato by inducing local resistance and increasing the fresh weight of tomato by producing IAA (Hu et al. 2022). We also evaluated differences in the soil fungal community compositions in soils treated with S, SC, and BC. The results suggest that S and SC treatments increase the abundance of some fungal species with plant disease biocontrol potential.

Conclusions

In this study, we identified and characterized the occurrence of *R. reniformis* on melon plants in China and compared the efficacy of several control strategies in the greenhouse. The findings of our study offer valuable insights into the potential damage caused by this nematode and provide useful information on effective control methods.

Methods

Plant and soil samples

In 2021–2022, some irregular stunted melon plants were observed in a greenhouse in the Jimo District (36.37°N; 120.51°E) of Qingdao, China. Roots of melon plants and rhizosphere soil were sampled and taken back to the Nematology Laboratory of Qingdao Agricultural University for identification.

The collection and observation of nematodes

Nematodes were extracted from the rhizosphere soil of melon plants using the Baermann tray method with some modifications (Barker 1985). The characteristics of immature females and males were observed and photographed by a compound microscope equipped with a Nomarski differential interference contrast (Axioscope 5, Zeiss, Germany). Measurements were performed using a drawing tube attached to the microscope. The females in the root tissue were stained using the sodium hypochlorite-acid fuchsin method (Byrd et al. 1983). Briefly, infected roots were placed in a beaker containing 50 mL of 1.5% NaOCl for 5 min, followed by washing with sterile water until all residual NaOCl had been removed. One milliliter of acid fuhsin was added to the beaker and incubated at 100°C in a water bath for 30 s. After washing with sterile water, the roots were placed in a beaker containing 20 mL of acid glycerol and boiled. Roots were then dissected, and the female nematodes were observed and photographed by a compound microscope (Axioscope 5, Zeiss, Germany).

Molecular characterization

DNA extraction and PCR

Genomic DNA was extracted from individual immature females according to previously described protocols with some modifications (Castagnone-Sereno et al. 1995; Holterman et al. 2006). In summary, a single nematode was transferred to a 0.2 mL PCR tube containing 10 μL of lysis buffer (60 mg/mL proteinase K, 40 mM NaCl, and 20 mM Tris-HCl at a pH of 8.0). Samples were incubated at 65°C for 90 min, followed by 95 °C for 10 min and then stored at -20°C for later use.

The D2–D3 region of the 28S rRNA gene and the ITS1 rRNA gene were amplified using the primer pairs D2A/D3B and TW81/AB28 (Additional file 2: Table S4). A total reaction volume of 25 μL was used for PCR. Each reaction contained 12.5 μL of I-5™ 2×High-Fidelity Master Mix (TSINGKE, China), 2 μL of template DNA, 2 μL of forward and reverse primers (10 μM), and 8.5 μL of nuclease-free water. The PCR cycling conditions were as follows: 98°C for 3 min (initial denature) followed by 30 cycles of 98°C for 10 s (denature), 55°C for 10 s (primer annealing), 72°C for 15 s (extension), and a final extension at 72°C for 5 min.

Sequencing and phylogenetic analyses
PCR products were purified using the E.Z.N.A. Gel Extraction Kit (Omega, USA) according to the manufacturer's instructions. Amplified fragments were cloned into the pClone007 Blunt Vector (TSINGKE, China) according to the manufacturer's instructions and sequenced in two primer directions by TSINGKE Biological Technology (Qingdao, China). The sequences obtained from the *R. reniformis* isolates were submitted to GenBank. Phylogenetic tree analyses were performed with MEGA7 software using the maximum likelihood method of 1000 replicates (Kumar et al. 2016).

Assessing the pathogenicity of *R. reniformis*
Egg masses of *R. reniformis* were hand-picked and placed in a petri dish. Eggs were then washed with 0.5% NaOCl for 1 min, followed immediately by five washes with sterile water. The egg masses were re-suspended in sterile water and incubated at 26°C for hatching. After 3 days, the newly hatched J2s were collected for melon plants inoculations. Melon seeds were surface sterilized with 1% NaOCl and germinated on moist filter paper. After 3 days, the germinated melon seeds were transferred to individual pots (9 cm×9 cm×10 cm) containing sterile substrate (70% peat and 30% vermiculite). Plants were cultivated at 26±3°C. When melon plants reached the two-leaf stage, we used a hole puncher to punch three small holes at a depth of 1 cm in the soil surrounding the root zone of each melon plant, and each hole was inoculated with 300 *R. reniformis* J2s in 1 mL of sterilized water, and then carefully covered with sterile substrate. Three days post-inoculation, the roots of melon plants were stained using acid fuchsin and observed under a stereoscope. Three independent experiments were carried out with similar results.

Greenhouse trial design
A greenhouse trial was carried out in Jimo in a greenhouse where we found the *R. reniformis*. Two greenhouse experiments were conducted from September to December 2021 and October to December 2022. The *R. reniformis* population densities in the greenhouse were detected before conducting the greenhouse experiments. The rhizosphere soil of each plot was sampled at five points, and 100 g of mixed soil from each point was used for nematode collection according to the Baermann tray method. *R. reniformis* was counted under a microscope (Olympus, Japan). Five treatments were applied: solarization [soil covered with high-density polyethylene film (0.2 mm; Shandong Xinyu Engineering Material Company Ltd.) during the whole month of August], fosthiazate (Fuqiduo; 10% fosthiazate granules; 80 g/plot), solarization followed by fosthiazate, solarization followed by chitooligosaccharide copper (Qingdao Zhongke Xinghai Biotechnology Co., Ltd; 5% chitooligosaccharide copper, 2.7% chelated copper; 200 mL/plot), and water (blank control). All treatments were arranged in a randomized complete blank design, and each treatment was applied to three replicated plots. Melon seedlings at the two-leaf stage were then transplanted in each plot. The area of each plot was 30 m², with four rows in each plot and 30 melon plants per row. The number of *R. reniformis* in the roots of melon plants and rhizosphere soil was recorded 3 days after the transplanting of melon seedlings. 28 days after the transplanting, five melon plants were randomly sampled from each plot (a total of 15 plants of each treatment), and growth parameters (shoot weight and shoot length) of melon plants were recorded. The temperature of the greenhouse was about 25–34°C. Thirty days after transplanting, the rhizosphere soil was collected for Illumina NovaSeq sequencing.

DNA extraction, Illumina NovaSeq sequencing, and analysis
An E.Z.N.A. Soil DNA Kit (Omega, USA) was used to extract DNA from rhizosphere samples according to the manufacturer's instructions. The DNA quantity and quality were evaluated using a NanoDrop 2000 spectrophotometer (Thermo Scientific, USA) and electrophoresis on a 1% agarose gel. The V3–V4 region of bacterial 16S rRNA and the ITS1 region of the fungal internally transcribed spacer were amplified using primer pairs 338F/806R and ITS1F/ITS2R (Additional file 2: Table S4). PCR products were purified using the EasyPure® Quick Gel Extraction Kit (TransGen, China) and sequenced on the Illumina Novaseq 6000 platform (Biomarker Technologies, China).

The bioinformatics analysis was performed using BMKCloud (http://www.biocloud.net/). Briefly, raw paired-end sequence reads were primarily filtered using Trimmomatic v0.33 (Bolger et al. 2014) and primer sequences were identified and removed using Cutadapt (Martin 2011). QIIME2 (Bolyen et al. 2019) and

Shi *et al. Phytopathology Research*   (2023) 5:58

Page 12 of 14

DADA2 (Callahan et al. 2016) were used to remove chimeric and short reads. Sequences with > 97% sequence similarity were clustered to one operational taxonomic units (OTUs) by USEARCH 10.0 (Rognes et al. 2016). For the microbial community analysis, alpha diversity indices, such as the Shannon index and ACE index (Lee et al. 1992; Spellerberg et al. 2003) were calculated using the picante database (Kembel et al. 2010). A beta diversity analysis was performed using qiime software (http://qiime.org/). A principal coordinates analysis (PCoA) (Gower 1966) was performed using R software (v4.1.2; http://www.r-project.org/). Significant differences in community structures among groups were assessed using an ANOVA followed by the Tukey's honest significant difference (HSD) tests. The phenotypic traits of microbial communities were predicted by BugBase (http://bugbase.cs.umn.edu).

Statistical analysis

Data derived from greenhouse experiments were analyzed for significance by one-way ANOVA followed by Duncan's multiple range test ($P \leq 0.05$) using the software SPSS (version 16.0 for Windows).

Abbreviations

ACE   Abundance-based richness estimation
ANOVA   Analysis of variance
BC   Blank control
F   Fosthiazate
PCoA   Principal coordinate analysis
PPN   Plant-parasitic nematodes
RN   *Rotylenchulus reniformis*
S   Soil solarization
SC   Combination of soil solarization and chitooligosaccharide copper
SF   Combination of soil solarization and fosthiazate

Supplementary Information

The online version contains supplementary material available at https://doi.org/10.1186/s42483-023-00217-6.

> **Additional file 1: Figure S1**. The symptoms of *R. reniformis* infected *C. melo* in the greenhouse of Jimo (Qingdao, China). Irregular stunted *C. melo* plants were detected in the sampling greenhouse. **Figure S2.** Evidence of the infection of *R. reniformis* in *C. melo* roots. Roots of *C. melo* plants were stained using acid fuchsin and observed under a stereoscope. Images were taken at **a** 4, **b** 7, **c** 10, and **d** 15 days post-inoculation (dpi). Scale bars = 50 μm. **Figure S3.** Analysis of alpha diversity and beta diversity of microbiota in the rhizosphere soil of *C. melo*.
>
> **Additional file 2: Table S1.** Effects of four treatments on growth parameters of *C. melo* infected with the *R. reniformis* in the greenhouse in Jimo (Qingdao, China) in 2021 and 2022. **Table S2.** The relative abundance of bacteria in the rhizosphere soil of *C. melo* at the genus level under different treatments. Each treatment included three replicates (S: soil solarization; SC: combination of soil solarization and chitooligosaccharide copper; BC: blank control). **Table S3.** The relative abundance of fungi in the rhizosphere soil of *C. melo* at the genus level under different treatments. Each treatment included three replicates (S: soil solarization; SC: combination of soil solarization and chitooligosaccharide copper; BC: blank control). **Table S4.** Primer sets used in the present study.

References
Agudelo P, Robbins RT, Stewart JM, Szalanski AL. Intraspecific variability of *Rotylenchulus reniformis* from cotton-growing regions in the United States. J Nematol. 2005;37(1):105–14.

Barker KR. Nematode extraction and bioassays. In: Barker KR, Carter CC, Sasser JN, editors. An advanced treatise on meloidogyne. Raleigh: North Carolina State University Graphics; 1985. p. 19–35.

Bolger AM, Lohse M, Usadel B. Trimmomatic: a flexible trimmer for Illumina sequence data. Bioinformatics. 2014;30(15):2114–20. https://doi.org/10.1093/bioinformatics/btu170.

Bolyen E, Rideout JR, Dillon MR, Bokulich NA, Abnet CC, Al-Ghalith GA, et al. Reproducible, interactive, scalable and extensible microbiome data science using QIIME 2. Nat Biotechnol. 2019;37(8):852–7. https://doi.org/10.1038/s41587-019-0209-9.

Byrd DW, Kirkpatrick T, Barker KR. An improved technique for clearing and staining plant tissues for detection of nematodes. J Nematol. 1983;15:142–3.

Callahan BJ, McMurdie PJ, Rosen MJ, Han AW, Johnson AJ, Holmes SP. DADA2: high-resolution sample inference from Illumina amplicon data. Nat Methods. 2016;13(7):581–3. https://doi.org/10.1038/nmeth.3869.

Cao H, Jiao Y, Yin N, Li Y, Ling J, Mao Z, et al. Analysis of the activity and biological control efficacy of the *Bacillus subtilis* strain Bs-1 against *Meloidogyne incognita*. Crop Prot. 2019. https://doi.org/10.1016/j.cropro.2019.04.021.

Castagnone-Sereno P, Esparrago G, Abad P, Leroy F, Bongiovanni M. Satellite DNA as a target for PCR specific detection of the plant-parasitic nematode *Meloidogyne hapla*. Curr Genet. 1995;28(6):566–70. https://doi.org/10.1007/BF00518170.

Castillo JD, Lawrence KS, Morgan-Jones G, Ramirez CA. Identification of fungi associated with *Rotylenchulus reniformis*. J Nematol. 2010;42(4):313–8.

Chellemi DO, Olson SM, Scott JW, Mitchell DJ, McSorley R. Reduction of phytoparasitic nematodes on tomato by soil solarization and genotype. J Nematol. 1993;25(4 Suppl):800–5.

Chen J, Li QX, Song B. Chemical nematicides: recent research progress and outlook. J Agric Food Chem. 2020;68(44):12175–88. https://doi.org/10.1021/acs.jafc.0c02871.

Davis RF, Koenning SR, Kemerait RC, Cummings TD, Shurley WD. *Rotylenchulus reniformis* management in cotton with crop rotation. J Nematol. 2003;35(1):58–64.

Elser JJ, Sterner RW, Gorokhova EA, Fagan WF, Markow TA, Cotner JB. Biological stoichiometry from genes to ecosystems. Ecol Lett. 2000;3(6):540–50. https://doi.org/10.1046/j.1461-0248.2000.00185.x.

Fan Z, Qin Y, Liu S, Xing R, Yu H, Li K, et al. Fluoroalkenyl-grafted chitosan oligosaccharide derivative: An exploration for control nematode *Meloidogyne incognita*. Int J Mol Sci. 2022;23(4):2080. https://doi.org/10.3390/ijms23042080.

Fan Z, Wang L, Qin Y, Li P. Activity of chitin/chitosan/chitosan oligosaccharide against plant pathogenic nematodes and potential modes of application in agriculture: a review. Carbohydr Polym. 2023;306: 120592. https://doi.org/10.1016/j.carbpol.2023.120592.

FAO. FAOSTAT. 2020. http://www.fao.org/faostat/en/#data. Accessed 3 Mar 2022.

Felsenstein J. Evolutionary trees from DNA sequences: a maximum likelihood approach. J Mol Evol. 1981;17:368–76. https://doi.org/10.1007/BF01734359.

Gower JC. Some distance properties of latent root and vector methods used in multivariate analysis. Biometrika. 1966;53(3–4):325–38. https://doi.org/10.2307/2333639.

Guan Z, Feng Q. Chitosan and chitooligosaccharide: the promising non-plant-derived prebiotics with multiple biological activities. Int J Mol Sci. 2022;23(12):6761. https://doi.org/10.3390/ijms23126761.

Gustavo RC, Torres GRC, Elvira MR, Pedrosa EMR, Kércya MS, Siqueira KMS. Response of Cucurbit species to *Rotylenchulus reniformis*. Fitopatol Bras. 2005;30:85–7.

Holterman M, Bongers T, Holovachov O. Phylum-wide analysis of SSU rDNA reveals deep phylogenetic relationships among nematodes and accelerated evolution toward crown clades. Mol Biol Evol. 2006;23(9):1798–800. https://doi.org/10.1093/molbev/msl044.

Hu Y, You J, Wang Y, Long Y, Wang S, Pan F, et al. Biocontrol efficacy of *Bacillus velezensis* strain YS-AT-DS1 against the root-knot nematode *Meloidogyne incognita* in tomato plants. Front Microbiol. 2022;13:1035748. https://doi.org/10.3389/fmicb.2022.1035748.

Jones JT, Haegeman A, Danchin EG, Gaur HS, Helder J, Perry RN, et al. Top 10 plant-parasitic nematodes in molecular plant pathology. Mol Plant Pathol. 2013;14(9):946–61. https://doi.org/10.1111/mpp.12057.

Kembel SW, Cowan PD, Helmus MR, Cornwell WK, Morlon H, Ackerly DD, et al. Picante: R tools for integrating phylogenies and ecology. Bioinformatics. 2010;26(11):1463–4. https://doi.org/10.1093/bioinformatics/btq166.

Koenning SR, Wrather JA, Kirkpatrick TL, Walker NR, Starr JL, Mueller JD. Plant-parasitic nematodes attacking cotton in the United States: old and emerging production challenges. Plant Dis. 2004;88(2):100–13. https://doi.org/10.1094/PDIS.2004.88.2.100.

Kumar S, Stecher G, Tamura K. MEGA7: molecular evolutionary genetics analysis version 7.0 for bigger datasets. Mol Biol Evol. 2016;33(7):1870–4. https://doi.org/10.1093/molbev/msw054.

Lee CSM. Estimating the number of classes via sample coverage. J Am Stat Assoc. 1992;87(417):210–7. https://doi.org/10.1080/01621459.1992.10475194.

Liu J, Li P, Yi C, Chen J, Tang C, Song Z. Occurrence of the reniform nematode *Rotylenchulus reniformis* on sponge gourd (Luffa cylindrica) in Yunnan province, China. Plant Dis. 2023a. https://doi.org/10.1094/PDIS-05-22-1147-PDN.

Liu Y, Yang H, Wen F, Bao L, Zhao Z, Zhong Z. Chitooligosaccharide-induced plant stress resistance. Carbohydr Polym. 2023b;302: 120344. https://doi.org/10.1016/j.carbpol.2022.120344.

Lopez-Nicora HD, Pedrozo LM, Grabowski OC, Orrego FA, Hahn VE, Ralston TI, et al. First report of the reniform nematode (*Rotylenchulus reniformis*) from soybean in paraguay. Plant Dis. 2018. https://doi.org/10.1094/PDIS-02-18-0240-PDN.

Maietti A, Tedeschi P, Stagno C, Bordiga M, Travaglia F, Locatelli M, et al. Analytical traceability of melon (*Cucumis melo* var *reticulatus*): proximate composition, bioactive compounds, and antioxidant capacity in relation to cultivar, plant physiology state, and seasonal variability. J Food Sci. 2012;77(6):C646–52. https://doi.org/10.1111/j.1750-3841.2012.02712.x.

Martin M. Cutadapt removes adapter sequences from high-throughput sequencing reads. Embnet J. 2011;17(1):10–2. https://doi.org/10.14806/ej.17.1.200.

Moura RM, Pedrosa EMR, Guimaraes LMP. Nematoses de alta importância econômica da cultura do melão no estado do Rio Grande do Norte. Brasil Fitopatol Bras. 2002;27:225 **(in Portuguese)**.

Nguyen HT, Trinh QP, Nguyen TD, Bert W. First report of *Rotylenchulus reniformis* infecting turmeric in Vietnam and consequent damage. J Nematol. 2020;52:1–5. https://doi.org/10.21307/jofnem-2020-053.

Noling JW, Becker JO. The challenge of research and extension to define and implement alternatives to methyl bromide. J Nematol. 1994;26:573–86.

Palomares-Rius JE, Cantalapiedra-Navarrete C, Archidona-Yuste A. Prevalence and molecular diversity of reniform nematodes of the genus *Rotylenchulus* (Nematoda: Rotylenchulinae) in the Mediterranean Basin. Eur J Plant Pathol. 2018;150(21):439–55. https://doi.org/10.1007/s10658-017-1292-8.

Pulavarty A, Egan A, Karpinska A, Horgan K, Kakouli-Duarte T. Plant parasitic nematodes: a review on their behaviour, host interaction, management approaches and their occurrence in two sites in the republic of Ireland. Plants (basel). 2021;10(11):2352. https://doi.org/10.3390/plants10112352.

Qing X, Bik H, Yergaliyev TM, Gu J, Fonderie P, Brown-Miyara S, et al. Widespread prevalence but contrasting patterns of intragenomic rRNA polymorphisms in nematodes: implications for phylogeny, species delimitation and life history inference. Mol Ecol Resour. 2020;20(1):318–32. https://doi.org/10.1111/1755-0998.13118.

Rebois RV. Effect of soil temperature on infectivity and development of *Rotylenchulus reniformis* on resistant and susceptible soybeans, *Glycine max*. J Nematol. 1973;5(1):10–3.

Rico X, Gullón B, Alonso JL, Yáñez R. Recovery of high value-added compounds from pineapple, melon, watermelon and pumpkin processing by-products: an overview. Food Res Int. 2020;132: 109086. https://doi.org/10.1016/j.foodres.2020.109086.

Ritschel PS, Lins TC, Tristan RL, Buso GS, Buso JA, Ferreira ME. Development of microsatellite markers from an enriched genomic library for genetic analysis of melon (*Cucumis melo* L.). BMC Plant Biol. 2004;4:9. https://doi.org/10.1186/1471-2229-4-9.

Robinson AF. Reniform in U.S. cotton: when, where, why, and some remedies. Annu Rev Phytopathol. 2007;45:263–88. https://doi.org/10.1146/annurev.phyto.45.011107.143949.

Robinson AF, Cook CG, Westphal A, Bradford JM. *Rotylenchulus reniformis* below plow depth suppresses cotton yield and root growth. J Nematol. 2005;37(3):285–91.

Rodriguez-Perez C, Quirantes-Pine R, Fernandez-Gutierrez A, Segura-Carretero A. Comparative characterization of phenolic and other polar compounds in Spanish melon cultivars by using high-performance liquid chromatography coupled to electrospray ionization quadrupole-time of flight mass spectrometry. Food Res Int. 2013;54(2):1519–27. https://doi.org/10.1016/j.foodres.2013.09.011.

Rognes T, Flouri T, Nichols B, Quince C, Mahé F. VSEARCH: a versatile open source tool for metagenomics. PeerJ. 2016;4: e2584. https://doi.org/10.7717/peerj.2584.

Savory EA, Granke LL, Quesada-Ocampo LM, Varbanova M, Hausbeck MK. The cucurbit downy mildew pathogen *Pseudoperonospora cubensis*. Mol Plant Pathol. 2011;12(3):217–26. https://doi.org/10.1111/j.1364-3703.2010.00670.x.

Schneider SM, Rosskopf EN, Leesch JG, Chellemi DO. United States Department of Agriculture-Agricultural Research Service research on alternatives to methyl bromide: pre-plant and post-harvest. Pest Manag Sci. 2003;59(6–7):814–26. https://doi.org/10.1002/ps.728.

Scholl EH, Thorne JL, McCarter JP, Bird DM. Horizontally transferred genes in plant-parasitic nematodes: a high-throughput genomic approach. Genome Biol. 2003;4(6):R39. https://doi.org/10.1186/gb-2003-4-6-r39.

Shao HD, Zhu LF, Li ZQ, Jiang R, Liu SM, Huang WK, et al. Population genetics of the cereal cyst nematode *Heterodera avenae* reveal geographical segregation and host adaptation. Phytopathol Res. 2023;5:30. https://doi.org/10.1186/s42483-023-00185-x.

Spellerberg IF, Fedor PJ. A tribute to Claude Shannon (1916–2001) and a plea for more rigorous use of species richness, species diversity and the "Shannon–Wiener" Index. Global Ecol Biogeogr. 2003. https://doi.org/10.1046/j.1466-822X.2003.00015.x.

Tian XL, Zhao XM, Zhao SY, Zhao JL, Mao ZC. The biocontrol functions of *Bacillus velezensis* strain Bv-25 against *Meloidogyne incognita*. Front Microbiol. 2022;13: 843041. https://doi.org/10.3389/fmicb.2022.843041.

Usovsky M, Lakhssassi N, Patil GB, Vuong TD, Piya S, Hewezi T, et al. Dissecting nematode resistance regions in soybean revealed pleiotropic effect of soybean cyst and reniform nematode resistance genes. Plant Genome. 2021;14(2): e20083. https://doi.org/10.1002/tpg2.20083.

Van Den Berg E, Palomares-Rius JE, Vovlas N, Tiedt LR, Castillo P. Morphological and molecular characterisation of one new and several known species of the reniform nematode, *Rotylenchulus* Linford & Oliveira, 1940 (Hoplolaimidae: Rotylenchulinae), and a phylogeny of the genus. Nematology. 2016;18(1):67–107.

Wubben MJ, Ganji S, Callahan FE. Identification and molecular characterization of a beta-1,4-endoglucanase gene (Rr-eng-1) from *Rotylenchulus reniformis*. J Nematol. 2010;42(4):342–51.

Yin N, Liu R, Zhao JL, Khan R, Li Y, Ling J, et al. Volatile organic compounds of *Bacillus cereus* strain Bc-cm103 exhibit fumigation activity against *Meloidogyne incognita*. Plant Dis. 2021;105(4):904–11. https://doi.org/10.1094/PDIS-04-20-0783-RE.

Zhang Y. Morphological, molecular and biological characteristics of *Rotylenchulus reniformis* occurring in China. 2010. Ph.D. thesis, Zhejiang University, Zhejiang, China **(in Chinese)**.

Zhou Y, Chen J, Zhu X, Wang Y, Liu X, Fan H, et al. Efficacy of *Bacillus megaterium* strain Sneb207 against soybean cyst nematode (*Heterodera glycines*) in soybean. Pest Manag Sci. 2021;77(1):568–76. https://doi.org/10.1002/ps.6057.